INTERNAL MEDICINE

□ CASE REPORT □

Two Cases of Neurolymphomatosis with Fatal Bilateral Vocal Cord Paralysis that were Diagnosed with ^{18}F-fluorodeoxyglucose Positron Emission Tomography (FDG PET)/CT

Yuichiro Ono[1], Yasuhiro Kazuma[2], Yotaro Ochi[2], Ryosuke Matsuoka[3], Yukihiro Imai[4] and Takayuki Ishikawa[1]

Abstract

Neurolymphomatosis is a rare entity defined as nerve infiltration by neurotropic abnormal lymphocytes which can lead to the development of neuropathy, with typical presentations including pain, hypoesthesia, paresthesis and palsy. We herein report two cases where critical bilateral vocal cord paralysis due to neurolymphomatosis in recurrent nerves occurred in refractory Burkitt lymphoma and adult T-cell lymphoma patients. High-dose methotrexate and intrathecal chemotherapy injection for the nervous lesions were ineffective, and the patients died. Neurolymphomatosis of the recurrent nerve is an emergent and difficult complication and should be suspected when sudden onset of aphasia, hoarseness or shortness of breath is found in refractory lymphoma patients.

Key words: vocal cord paralysis, neurolymphomatosis, recurrent laryngeal nerve, Burkitt lymphoma, adult T-cell leukemia

(Intern Med 56: 1193-1198, 2017)
(DOI: 10.2169/internalmedicine.56.6998)

Introduction

Neurolymphomatosis is a rare complication of hematological malignancies, especially non-Hodgkin lymphoma derived from B- and T-cells, which is caused by direct invasion of abnormal lymphocytes and develops neurological manifestations (1). Although central nervous system-directed chemotherapy, including high-dose methotrexate and cytarabine, intracranial fluid chemotherapy infusion and radiotherapy, are used in clinical settings, the efficacy is unsatisfactory, and it is difficult to control the insidious symptoms by treatment and expert palliative care. Additionally, it is extremely challenging to diagnose neurolymphomatosis itself, partly because there is no diagnostic modality with satisfactory sensitivity. A biopsy of the lesion is the gold standard, but it is not always possible to acquire a sufficiently substantial histological specimen. Recently, attention has been focused on magnetic resonance imaging (MRI) and ^{18}F-fluorodeoxyglucose (FDG)-positron emission tomography (PET) combined with computed tomography (CT) as sensitive and noninvasive diagnostic modalities for neurolymphomatosis, which may be useful alternatives to a biopsy (2, 3).

Burkitt lymphoma is a highly aggressive B-cell non-Hodgkin lymphoma characterized by translocation between the MYC gene on chromosome 8 and the IGH gene on chromosome 14, the IGK gene on chromosome 2, or the IGL gene on chromosome 22. Burkitt lymphoma often involves extra-nodal sites including the central nervous system, ileocecal region, ovaries, and kidneys (4). Bone marrow involvement (up to 70%) and leptomeningeal involvement (up to 40%) are common findings at the diagnosis (5-8), and central nervous system prophylaxis measure-combined sys-

[1]Department of Hematology, Kobe City Medical Center General Hospital, Japan, [2]Department of Hemato-oncology, Kyoto University, Japan, [3]Department of Pathology, Kobe City Medical Center General Hospital, Japan and [4]Department of Clinical Pathology, Kobe City Medical Center General Hospital, Japan

Received for publication December 17, 2015; Accepted for publication September 4, 2016

Correspondence to Dr. Yuichiro Ono, u1ax.ono@gmail.com

temic chemotherapy is recommended. The 2-year event-free survival range for these regimens is 64-95%.

Adult T-cell leukemia (ATL) is defined as a peripheral T-cell neoplasm associated with infection of human T-cell leukemia virus type 1 (HTLV-1), according to the World Health Organization classification 2008. Acute-type ATL is the most aggressive of four variants (smoldering type, chronic type, lymphoma type, and acute type), and the characteristic clinical presentations are organomegaly, lymphadenopathy, an elevated lactate dehydrogenase level, hypercalcemia, and circulating malignant cells (4). It was reported that central nervous system involvement was more common in ATL than in other lymphoma types (9). The median survival rate with an aggressive combination regimen is 13 months, and the overall survival rate at 3 years is 24% (10).

Both entities of aggressive lymphoma can recur in the central nervous system, at which point they often not only spread into the cerebrospinal fluid and attach to the meninges, or coat nerve fibers (lymphomatous meningitis), but also infiltrate into the peripheral and cranial nerves (neurolymphomatosis).

We herein report two rare cases of sudden onset of dysphasia and fatal respiratory distress attributed to neurolymphomatosis that was diagnosed with ^{18}F-FDG PET.

Case Reports

Case 1

A 39-year-old man was referred to our hospital because of malignant lymphoma that was diagnosed after a biopsy of the stomach. The patient presented to our outpatient unit with a stomach ache and anorexia. A physical examination revealed no epigastric tenderness but did show hypoesthesia of the right lower quadrant abdomen and back (at the levels of Th10-Th12) and the distal portion of the left arm. Contrast CT showed soft tissue density in the hilus of the right kidney, the upper portion of the right ureter, the pancreatic tail, the area between the left clavicle and the right intervertebral foramen, along the right iliopsoas, and the root of the superior mesenteric artery. ^{18}F-FDG PET/CT showed an intense uptake in the above lesions and the bilateral testes and a weak uptake around the pancreas tail and along the right ileopsoas, suggesting lymphoma lesions.

The white blood count was 8,400/μL, the alanine transferase level was 67 IU/L (standard range, 8-40 IU/L), the aspartate transferase level was 34 IU/L (standard range, 8-40 IU/L), the lactate dehydrogenase level was 516 IU/L (standard range, 120-250 IU/L), the alkaline phosphatase level was 578 IU/L (standard range, 100-340 IU/L), the creatinine level was 0.79 mg/dL (standard range, 0.4-0.8 mg/dL), the blood urea nitrogen level was 14.7 mg/dL (standard range, 8-20 mg/dL), and the soluble interleukin 2 receptor level was 3,183 IU/mL (standard range, 220-530 IU/mL). A histological examination of the stomach revealed a diffuse monotonous pattern of middle-sized lymphocytes whose nuclei were round with dispersed chromatin. Immunohistochemical staining revealed that the abnormal lymphocytes were positive for CD10, CD20, and Ki-67 (98%) and were negative for BCL2. Fluorescence *in situ* hybridization revealed that the lymphocytes were positive for split signals of the chromosomal region 8q24 (Vysis® LSI MYC Break Apart Rearrangement Probe Kit, Abbott, Abbottpark, USA). In the cerebrospinal fluid, CD5-, CD10+, CD19+, CD20+, and λ+ abnormal lymphocytes were found, and a polymerase chain reaction detected monoclonal rearrangement of immunoglobulin heavy chain. Meningeal dissemination of the lymphoma was suspected; thus, stage IV Burkitt lymphoma was diagnosed.

Following the infusion of 80 mg of methylprednisolone, a hyperfractionated cyclophosphamide, vincristine, adriamycin, and dexamethasone plus rituximab regimen with alternating high-dose methotrexate and cytarabine (HD-MA) and concurrent intrathecal infusion of methotrexate, cytarabine, and prednisolone was started. Following one cycle of chemotherapy (on day 44 after the diagnosis), no significant ^{18}F-FDG uptake in the abovementioned lesions was found, and abnormal lymphocytes disappeared from the cerebrospinal fluid. However, during the second cycle, abnormal lymphocytes reappeared in the cerebrospinal fluid.

The patient complained of hoarseness on day 68; however, the hoarseness improved spontaneously after a few days. On day 98, blurred vision in the left eye arose and gradually worsened. Contrast MRI revealed left optic nerve thickening, which was considered to reflect the involvement of the lymphoma. Loco-regional radiotherapy of the left optic nerve was started on day 102 with palliative intent. At that time, hoarseness recurred, and laryngoscopy showed bilateral vocal cord semi-paralysis. PET/CT on day 106 showed an uptake in the macule of the left eye, along the left jugular vein [maximum standardized uptake value (SUVmax), 19.6], at the left roots of the nerves at C4/5 and C5/6 (SUVmax, 13.4), and along the recurrent nerve at the arch of the aorta (Fig. 1a-d). The following day, the hoarseness worsened with onset of dysphagia and left shoulder pain. Despite loco-regional radiotherapy for the aorta and the left roots of the nerves at C4-C6, his symptoms deteriorated rapidly. He lost left-sided visual activity within a few days and died of systemic lymphoma invasion and bacterial pneumonia on day 138.

An autopsy showed a substantial invasion of abnormal lymphocytes into the neural fascicles of the left brachial plexus and bilateral cranial nerves comprising the optic, oculomotor, trochlear, trigeminal, abducens, facial, vestibulocochlear, glossopharyngeal and vagus nerves (Fig. 1g-j). The histopathology at the diagnosis is shown in Fig. 1e-f. In the brachial plexus, abnormal lymphocytes invaded diffusely among the neural nerves. In the brain, there were abnormal lymphocytes in the perivascular and parameningeal spaces, but not in the parenchyma. The left recurrent nerve with the ^{18}F-FDG uptake at the aortic arch could not be identified on the autopsy. Postmortem histopathology revealed other in-

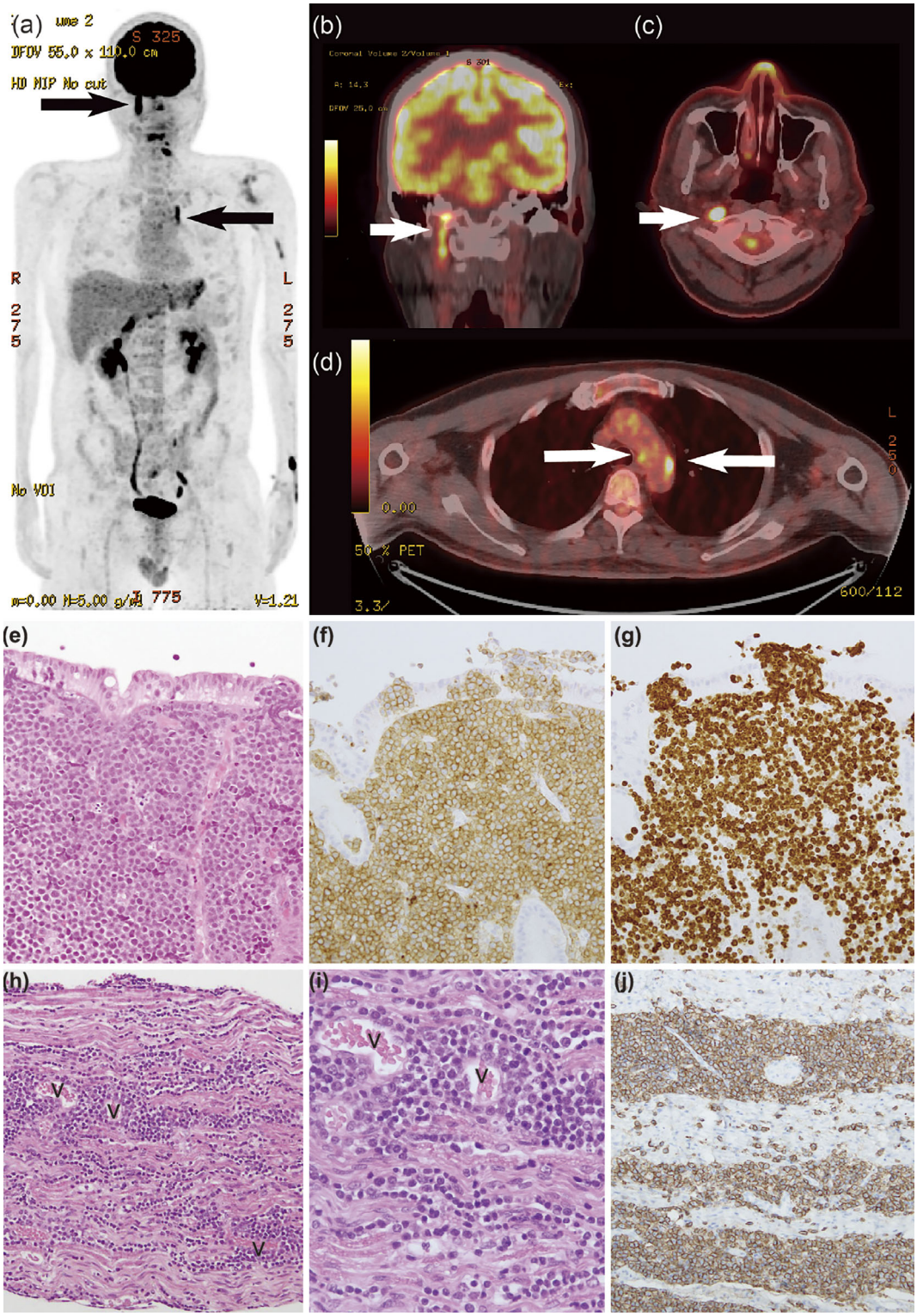

Figure 1. **a) ^{18}F-FDG PET in the maximum intensity projection, b) PET/CT fusion images showing the right vagal nerve involvement, shown as a linear uptake, c) PET/CT fusion images at the levels of the mesopharynx and d) arch of the aorta. White and black arrows represent the ^{18}F-FDG uptake in the right vagus nerve and left recurrent nerve. e) A pathological study at the diagnosis of the stomach [Hematoxylin and Eosin (H&E) staining, 20×], f) A pathological study at the diagnosis of the stomach (CD10 staining, 20×), g) A pathological study at the diagnosis of the stomach (Ki-67, 20×). h) A postmortem pathological study of the right vagus nerve (originating portion from the medulla) (H&E staining, 10×), i) A postmortem pathological study of the right vagus nerve (originating portion from the medulla) showing abnormal lymphocyte involvement around the vessels and into the nerve fiber bundle (H&E staining, 40×), j) A postmortem pathological study of the same specimen as in h, showing obviously stained lymphocytes (CD20, 40×). "v" denotes vessels in the tissue.**

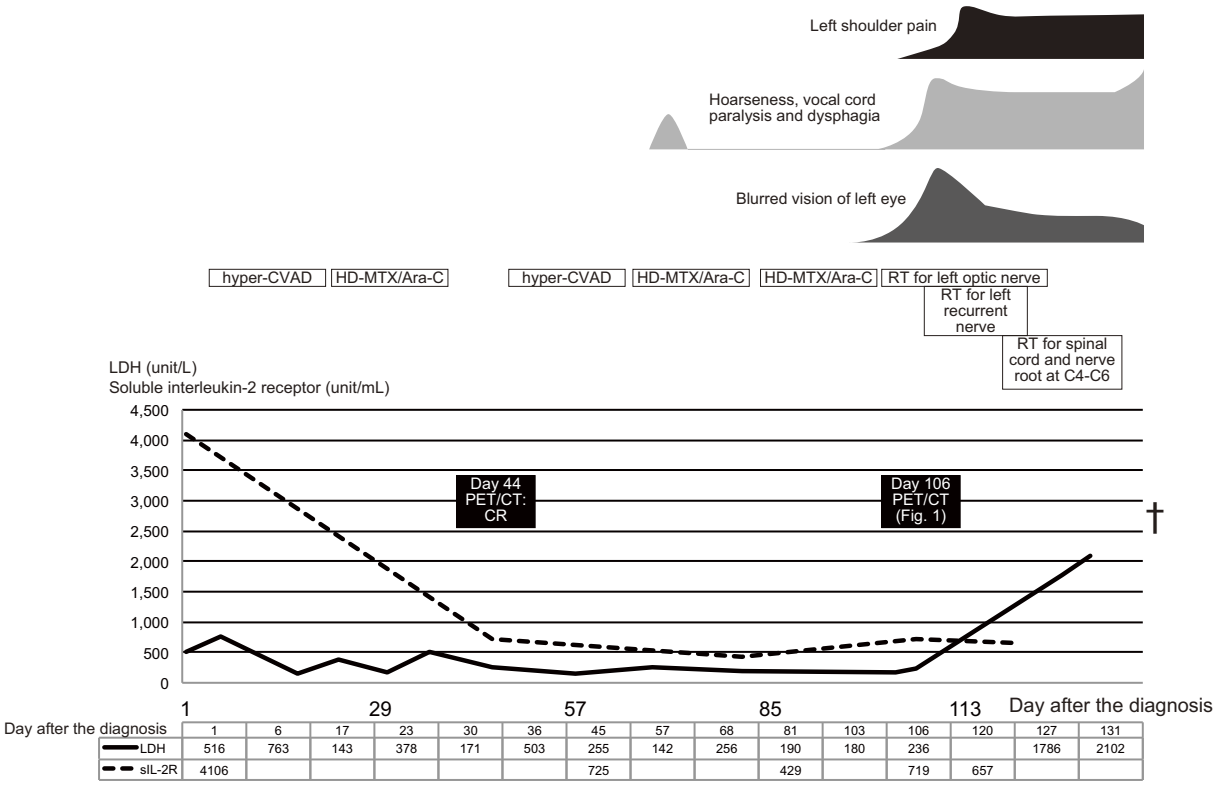

Figure 2. The clinical course of Case 1, including the symptoms, the treatment, and the laboratory data. Hyper-CVAD: hyperfractionated cyclophosphamide, vincristine, doxorubicin, and dexamethasone regimen, HD-MTX/Ara-C: high-dose methotrexate and cytarabine regimen, RT: radiotherapy, PET/CT: positron emission tomography combined with computed tomography, LDH: leucine dehydrogenase

volved organs, including the liver, kidneys, ureter, testis, and pituitary gland. The clinical course of Case 1 is shown in Fig. 2.

Case 2

A 48-year-old woman was referred to our hospital because of edematous erythema of the chest, back, and thighs that was refractory to topical steroid ointment. CT showed enlarged lymph nodes in the neck, axillae, lesser curvature of the stomach, and periaortic and inguinal regions. The white blood cell count was 27,100/μL, of which 80% were lymphocytes with hyperlobulated nuclei. Flow cytometric immunophenotyping showed the lymphocytes were CD4+, CD7-, CD8-, CD25+, and CD26-. Serum HTLV-1 antibody was positive, and Southern blotting revealed monoclonal integration of the HTLV-1 provirus genome, confirming the diagnosis of acute-type ATL.

After two courses of an intensive chemotherapy regimen comprising cyclophosphamide, adriamycin, vincristine, vinblastine, ranimustine, etoposide, paraplatin, and prednisolone (8), the involved nodes shrank, and the rash promptly resolved. Around day 90 after the diagnosis, the skin lesion recurred, accompanied by dysesthesia of the feet and diplopia of the right eye. A cerebrospinal fluid analysis showed central nervous system involvement, as manifested by the presence of atypical lymphocytes with the same immunophenotype as at the first presentation. After just two courses of high-dose methotrexate, the symptoms were temporarily ameliorated; however, around day 110 after the diagnosis, there was new onset of dysesthesia of the hands, which extended proximally. On day 114 after the diagnosis, the patient complained of hoarseness and sudden breathing difficulty. Laryngoscopy showed bilateral immotile folds, and bilateral vocal cord paralysis was diagnosed, with emergency tracheotomy performed. MRI of the brain and spinal cord was unremarkable. A cerebrospinal fluid sample was not obtained because we did not receive consent from the patient. However, ^{18}F-FDG PET demonstrated a significant FDG uptake in the sciatic and iliac nerves, lower cervical nerve plexuses, pituitary gland, skin, mammary glands, and region along the recurrent nerves (Fig. 3). On day 134 after the diagnosis, the patient died because of hypopnea due to paralysis of the respiratory muscles. An autopsy was not performed. The clinical course of Case 2 is shown in Fig. 4.

Discussion

The rare involvement of abnormal lymphocytes with bilateral vagus nerves causing vocal cord paralysis was found in the postmortem histopathology of Case 1. To our knowledge, this is the first case of bilateral vocal cord paralysis due to neurolymphomatosis where the histologic findings

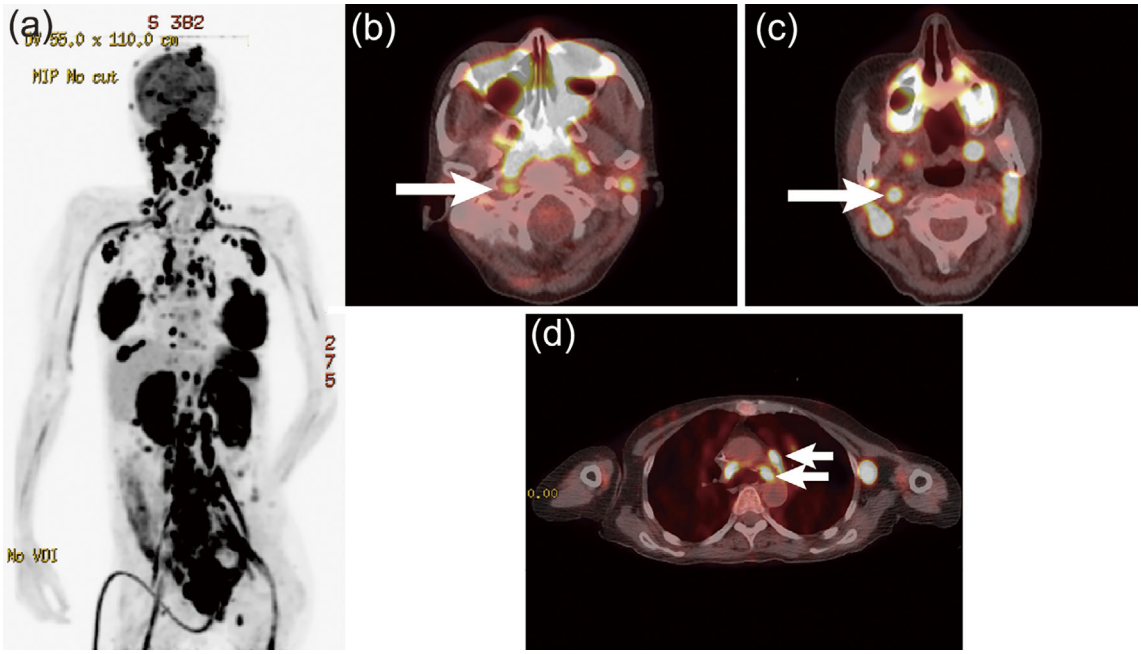

Figure 3. a) ^{18}F-FDG PET in the maximum intensity projection and b) PET/CT fusion images at the levels of the mesopharynx and c) arch of the aorta. The arrows represent the ^{18}F-FDG uptake in the right vagus nerve and left recurrent nerve of Case 2.

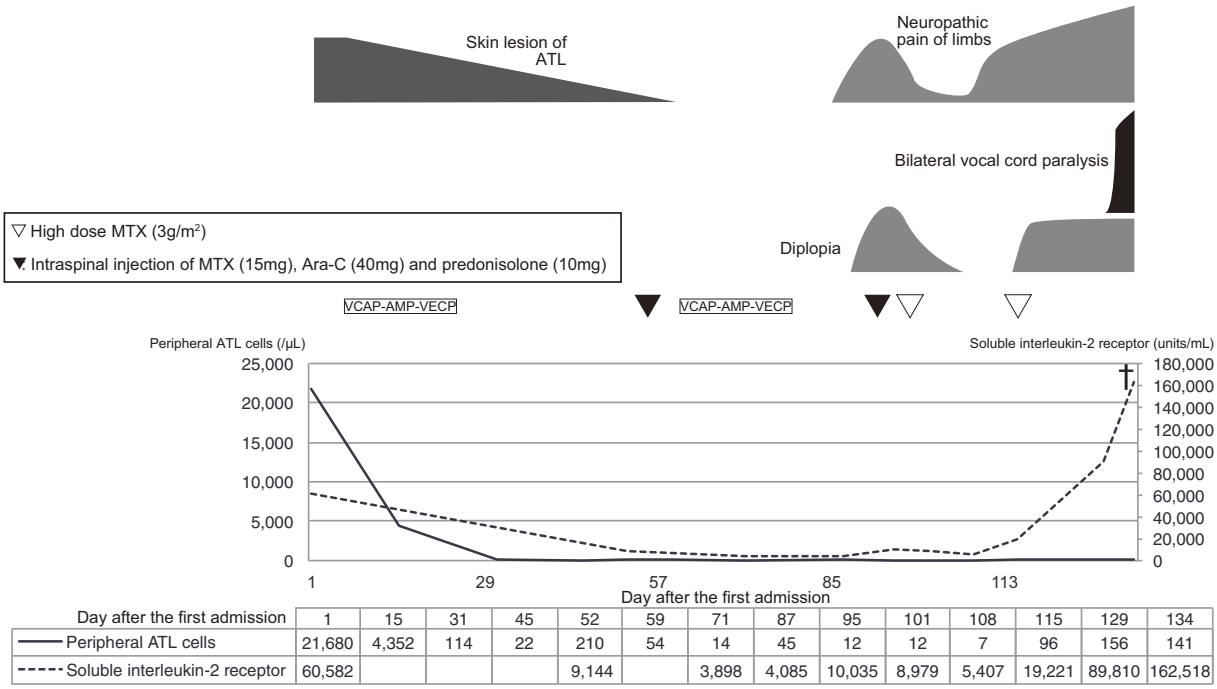

Day after the first admission	1	15	31	45	52	59	71	87	95	101	108	115	129	134
Peripheral ATL cells	21,680	4,352	114	22	210	54	14	45	12	12	7	96	156	141
Soluble interleukin-2 receptor	60,582				9,144		3,898	4,085	10,035	8,979	5,407	19,221	89,810	162,518

Figure 4. The clinical course of Case 2, including the symptoms, the treatment, and the laboratory data. VCAP-AMP-VECP: cyclophosphamide, adriamycin, vincristine, vinblastine, ranimustine, etoposide, paraplatin and prednisolone regimen, MTX: methotrexate, Ara-C: cytarabine, ATL: adult T-cell leukemia

are shown.

It is often challenging to diagnose neurolymphomatosis due to its non-specific presentation and the low sensitivity of the modalities available for diagnosis. The clinical presentation was described by Gan et al. (1) as follows: the painful involvement of nerves or roots, cranial neuropathy with or without pain, the painless involvement of peripheral nerves, and the painful or painless involvement of a single peripheral nerve. Neurolymphomatosis is highly suspected upon presentation of conditions including plexopathy, mononeuritis multiplex, footdrop, radiculopathy, and cranial nerve palsy. However, diverse differential diagnoses should

be considered, such as leptomeningeal lymphomatosis, nerve damage from herpes zoster, chemotherapy-induced neuropathy, nerve root compression, radiotherapy-induced neuropathy, lymphoma-associated vasculitis, and paraneoplastic syndrome.

The available diagnostic modalities for neurolymphomatosis other than a biopsy are a cerebrospinal fluid analysis and imaging, including MRI and ^{18}F-FDG PET. Some studies have reported that ^{18}F-FDG PET may be more sensitive than MRI based on a systematic review (9, 10). For example, Baehring et al. reported that the sensitivity of MRI for neurolymphomatosis detection was 40% (3), whereas Grisariu et al. reported that the sensitivities of MRI and ^{18}F-FDG PET were 78% and 87.5%, respectively (11). The sensitivity of ^{18}F-FDG PET is not 100%; as such, a multidisciplinary approach for an accurate diagnosis in patients with highly suspected neurolymphomatosis is warranted.

In Case 1, ^{18}F-FDG PET showed a linear uptake along the right vagus nerve running down into the carotid artery sheath and the left recurrent nerve at the level of the aortic arch. The autopsy histopathology showing involvement of the liver, kidney, and other regions with abnormal lymphocytes was discordant with the ^{18}F-FDG PET findings. This is likely due to the time gap between the ^{18}F-FDG PET imaging and the autopsy.

In Case 2, while MRI did not demonstrate findings of neurolymphomatosis, such as abnormal enhancement and thickness of the involved nerves, ^{18}F-FDG PET showed an uptake at part of the right vagus nerve running down into the right carotid artery sheath and at part of the left recurrent nerve at the level of the aortic arch.

In conclusion, we found that ^{18}F-FDG PET/CT is useful for the differential diagnosis of bilateral vocal cord paralysis in aggressive lymphoma patients, even when MRI is unrevealing, and that bilateral vocal cord paralysis due to neurolymphomatosis can be very aggressive and fatal if the causative hematological malignancy is resistant to treatment, including chemotherapy and radiation therapy.

The authors state that they have no Conflict of Interest (COI).

Acknowledgement

We thank H.M. and N.K. for their analysis of the multiparametric flow cytometry findings.

References

1. Gan HK, Azad A, Cher L, Mitchell PLR. Neurolymphomatosis: diagnosis, management, and outcomes in patients treated with rituximab. Neuro-oncology **12**: 212-215, 2010.
2. Salm LP, Van der Hiel B, Stokkel MPM. Increasing importance of ^{18}F-FDG PET in the diagnosis of neurolymphomatosis. Nucl Med Commun **33**: 907-916, 2012.
3. Toledano M, Siddiqui MA, Thompson CA, Garza I, Pittock SJ. Teaching NeuroImages: diagnostic utility of FDG-PET in neurolymphomatosis. Neurology **81**: e3, 2013.
4. Leoncini L, Raphaël el M, Stein H, Harris NL, Jaffe ES, Kluin PM. Burkitt lymphoma. In: WHO Classification of Tumours of Haematopoietic and Lymphoid Tissues. IARC, Lyon, 2008: 262-264.
5. Blum KA, Lozanski G, Byrd JC. Adult Burkitt leukemia and lymphoma. Blood **104**: 3009-3020, 2004.
6. Ferry JA. Burkitt's lymphoma: clinicopathologic features and differential diagnosis. Oncologist **11**: 375-383, 2006.
7. Sariban E, Edwards B, Janus C, Magrath I. Central nervous system involvement in American Burkitt's lymphoma. J Clin Oncol **1**: 677-681, 1983.
8. Zelenetz AD, Gordon LI, Wierda WG. NCCN Clinical Practice Guidelines in Oncology. 2nd ed [Internet]. [cited 2015 Apr 30] National Comprehensive Cancer Network, 2015: 1-463. Available from: http://www.nccn.org/professionals/physician_gls/pdf/nhl.pdf
9. Teshima T, Akashi K, Shibuya T, et al. Central nervous system involvement in adult T-cell leukemia/lymphoma. Cancer **65**: 327-332, 1990.
10. Tsukasaki K, Utsunomiya A, Fukuda H, et al. VCAP-AMP-VECP compared with biweekly CHOP for adult T-cell leukemia-lymphoma: Japan Clinical Oncology Group Study JCOG9801. J Clin Oncol **25**: 5458-5464, 2007.
11. Grisariu S, Avni B, Batchelor TT, et al. Neurolymphomatosis: an International Primary CNS Lymphoma Collaborative Group report. Blood **115**: 5005-5011, 2010.